Published in final edited form as:
Cancer. 2010 November 1; 116(21): 5093–5101. doi:10.1002/cncr.25260.

Sequential MR Imaging of Cervical Cancer: Predictive Value of Absolute Tumor Volume and Regression Ratio Measured before, during and after Radiation Therapy

Jian Z. Wang, Ph.D.[1], **Nina A. Mayr, M.D.**[1], **Dongqing Zhang, Ph.D.**[1], **Kaile Li, Ph.D.**[1], **John C. Grecula, M.D.**[1], **Joseph F. Montebello, M.D.**[1], **Simon S. Lo, M.D.**[1], and **William T.C. Yuh, M.D., M.S.E.E.**[2]

[1]Department of Radiation Medicine The Ohio State University, Columbus, OH 43210

[2]Department of Radiology The Ohio State University, Columbus, OH 43210

Abstract

Background—To investigate outcome prediction by measuring tumor absolute volume and regression ratio using serial magnetic resonance imaging (MRI) during radiation therapy (RT) of cervical cancer and to develop algorithms identifying patients at risk of poor therapeutic outcome.

Methods—Eighty patients with cervical cancer stages IB_2-IVA underwent 4 MRI scans: pre-RT, during RT at 2-2.5 weeks and 4-5 weeks, and at 1-2 months after RT. Median follow-up was 6.2 (range 0.2-9.4) years. Tumor volumes (V_1, V_2, V_3, V_4) and tumor regression ratios (V_2/V_1, V_3/V_1, V_4/V_1) were measured by 3D volumetry. Predictive metrics based on tumor volume/regression parameters were correlated with ultimate clinical outcome, including tumor local recurrence (LR) and patient dead of disease (DOD). Predictive power was evaluated using the Mann-Whitney test, sensitivity/specificity, and Kaplan-Meier analyses.

Results—Both tumor volume and regression ratio correlated strongly with LR (p=0.06, 5×10^{-4}, 1×10^{-6}, 2×10^{-8} for V_1, V_2, V_3, V_4; p=7×10^{-5}, 1×10^{-6}, 1×10^{-8} for V_2/V_1, V_3/V_1, V_4/V_1, respectively) and DOD (p=0.015, 0.004, 0.001, 3×10^{-4} for V_1, V_2, V_3, V_4; p=0.03, 0.009, 3×10^{-4} for V_2/V_1, V_3/V_1, V_4/V_1, respectively). Algorithms combining tumor volumes and regression ratios improved predictive power (sensitivity 61%–89%, specificity 79%–100%). The strongest predictor, pre-RT volume and regression ratio at the 3rd MRI ($V_1>40cm^3$ and $V>_3/V_1>20\%$), achieved 89% sensitivity, 87% specificity, and 88% accuracy for LR, 54% sensitivity, 83% specificity and 73% accuracy for DOD.

Conclusion—These results suggest that tumor volume/regression parameters are useful in predicting LR and DOD after primary therapy. As early outcome predictors, both tumor volume and regression ratio provide important information that may guide early intervention for patients at high risk of treatment failure.

Keywords

Cervical cancer; MR imaging; Absolute tumor volume; Tumor regression ratio; Tumor local control; Patient disease-specific survival

Requests for reprints: William T.C. Yuh M.D. Department of Radiology, The Ohio State University, 395 West 12th Ave, Suite 489, Columbus, Ohio 43210. Phone: 614-293-8299; Fax: 614-366-0743; William.Yuh@osumc.edu. .

Financial disclosure: None.

Introduction

The ability of magnetic resonance imaging (MRI) to differentiate tumor from normal soft tissue and to delineate tumor extent with high precision has greatly improved the quantitative assessment of tumor volume in cervical cancer [1-4]. Pretreatment tumor volume, a well-known prognostic factor in cervical cancer[5-8], can now be measured much more accurately using three-dimensional (3D) quantitative volumetry of the tumor with the improved lesion contrast and the multiplanar imaging ability of MRI. In addition, subtle volume changes during early therapy can be monitored closely as an early indicator of tumor response to an ongoing treatment. Irregular tumor shape and non-linear treatment-related shrinkage make it difficult to identifying such subtle changes using traditional methods, which measure only one- or two-dimensional maximal diameters of the tumor. This challenge can be overcome by quantitating detailed temporal changes of tumor volume using 3D volumetry using serial MRI during the course of radiation and chemotherapy (RT/CT).

Early results evaluating this new 3D imaging-based information suggest that therapy-induced tumor volume changes can be predictive of ultimate tumor local control and patient survival [5-8]. Various tumor parameters and time points for MRI measurements have been suggested for outcome prediction, including pre-, during, and post-therapy follow-up [9-13]. However, the simple practical paradigm and parameter thresholds for clinical implementation based upon such large and varied quantity of imaging data, including the imaging timing, has not been well defined or validated clinically with a long-term clinical study.

The purpose of this study was to investigate the efficacy of outcome prediction using serial MRI examinations to measure both tumor volumes and regression ratios before, during, and after RT/CT and to develop algorithms to identify cervical cancer patients at risk of treatment failure.

Materials and Methods

Patient population and treatment

Eighty patients with cervical cancer stages IB_2-IVA were treated with standard RT/CT on an IRB approved imaging study. Informed consent was obtained from all patients included in this study. Patient ages ranged from 25 to 85 years (median 51 years). RT consisted of standard external-beam RT (EBRT) plus lowdose-rate (LDR) brachytherapy. The dose prescription was 45-50 Gy of EBRT delivered in daily fractions of 1.8-2 Gy and 40 Gy of LDR brachytherapy delivered in 2 fractions of 20 Gy. Median follow up was 6.2 years (range 0.2-9.4 years).

MR imaging protocol

The imaging protocol included serial MRI studies at four welldefined time points: (1) MRI1 at the beginning of RT, (2) MRI2 early during RT (2-2.5 weeks with a RT dose of 20-25 Gy), (3) MRI3 midway during RT (4-5 weeks with 45-50 Gy), and (4) MRI4 at the follow-up visit (1-2 months after the completion of all therapy).

The MRI examinations were conducted using a standard body coil with a 1.5 Tesla superconductive scanner including Signa (General Electric Medical Systems, Milwaukee, WI) and Siemens Vision (Siemens Medical, Inc., Erlangen, Germany). The change in platforms was necessitated by a change in imaging systems at our institutions. Imaging included sagittal 5 mm (4 mm thickness with a 1 mm gap) conventional fast spin echo T2-weighted images (TE_{eff} =104, TR=4000, ETL=10, NEX=2) and axial 7 mm (5 mm

thickness with a 2 mm gap) T2-weighted and T1-weighted images (TE=16, TR=600, NEX=2). No MRI was performed with dwelling brachytherapy applicators.

Only patients who completed all 4 MRI studies were included in this study. Of a total of 115 patients, 80 patients completed the four MRIs, and these constitute the cohort of this study. The therapy was standard RT/CT for patients with cervical cancer and not influenced by the imaging findings.

Tumor volume and temporal change

The imaging data sets were evaluated by three reviewers, two MRI radiologists (14 and 10 years of experience) and one radiation oncologist (10 years of experience in MRI-based RT planning).

The tumor was defined as abnormal area with intermediate to high signal intensity on T2-weighted images with respect to the surrounding cervical stroma and uterus, and lower than the fluid signal in the urinary bladder [1, 12, 14]. Discrepancies in tumor delineation among the reviewers were resolved by consensus. For the 3D volumetry, the region-of-interest (ROI) was delineated on each imaging slice on the sagittal T2-weighted image, and the 3D ROI-based volumes were then calculated by the summation of all tumor areas and multiplication by the slice thickness. More recently we also have calculated tumor volumes separately using pixel summation and we found consistent results. Our developed code for image data analysis was based on MATLAB platform (MATLAB R2006a, MathWorks Inc., Natick, MA).

Statistical analysis

Tumor volumes (V_1, V_2, V_3, and V_4) measured by MRI 3D volumetry at time points of MRI1, MRI2, MRI3, and MRI4 were used to compute the regression ratios (V_2/V_1, V_3/V_1, and V_4/V_1) for each patient. Both tumor volume and regression ratio data were correlated with patient outcome endpoints, tumor local recurrence (LR) and dead of disease (DOD) based on clinical follow-up. LR in the pelvis was defined as tumor re-growth or persistence of tumor in the cervix after treatment completion. Cases other than LR were considered as local control (LC) of tumor. For DOD, death from cervical cancer or cancer complications was scored as event, and death from intercurrent disease was censored. Patients other than DOD were considered as disease-specific survival (DSS). The correlation between the volume and ratio parameters and the outcome of LR and DOD were performed using the Mann-Whitney rank-sum test [15].

Receiver Operating Characteristics (ROC) analysis was performed to define the best cut-off for each volume and regression ratio. The resulting parameter cut-offs to differentiate poor from favorable outcome groups were then subjected to sensitivity/specificity analysis, Kaplan-Meier actuarial life table analysis, and log-rank tests so that improved prediction algorithms could be established by combining the predictive powers of volumes and regression ratios at various time points. All statistical analyses were performed on the SPSS (SPSS 16, SPSS Inc. Chicago, IL).

Results

Tumor volume and regression ratio

Mean, range and standard deviations of the serial V_1, V_2, V_3, and V_4 are summarized in Table 1 for two outcome groups for all patients. Based on the measurements of the 80 patients included in this study, the mean initial tumor volume (V_1) was 80.5 cm^3 and varied widely from 3.4 to 700 cm^3. During therapy, the tumor volume regressed approximately in

an exponential fashion with mean regression ratios of 56%, 18%, and 5% for V_2/V_1, V_3/V_1, and V_4/V_1 measured in MRI2, MRI3, and MRI4, respectively. Overall, the mean tumor volumes and standard deviations were much smaller in the tumor local control (LC) and disease-specific survival (DSS) groups.

Prediction power of individual MRI studies

The overall tumor LC rate for the 80 patients was 78% and the DSS rate was 65%. The prediction power of parameters from all 4 MRI studies for LC and for DSS is presented in Table 2. All tumor volumes (V_2, V_3, and V_4), except for V_1 and all the regression ratios (V_2/V_1, V_3/V_1, and V_4/V_1) correlated significantly with LC with p-values ranging from 5×10^{-4} to 1×10^{-8} and DSS (p-values ranging from 0.015 to 3×10^{-4}) (Table 2). Based upon the p-value, V_1 is least significant for predicting therapy outcome when compared with the rest of the MRI predictors.

Because of the large variation of the tumor stage (ranged from IB_2 to IVA) and the initial tumor size (V_1 ranged from 3.4 cm^3 to 700 cm^3), we further stratified the patient population into two groups based on tumor stage: 42 patients had Stage I-II (Group 1) and 38 patients had Stage III & IVA (Group 2). The initial tumor volume (V_1) had a mean of 53 cm^3 and a range from 3.4 cm^3 to 259 cm^3 for Group 1, compared to a mean of 111 cm^3 and a range from 24 cm^3 to 700 cm^3 for Group 2. The difference of V_1 between the two groups was significant (p=0.008). The prediction values of the volume parameters for the two groups are presented in Table 2. The trend of the p-values for each stage group was overall consistent with that of the entire patient group, although the prediction power was not as significant as that of the entire patient population because of the smaller patient numbers in each group.

Similarly we examined the prediction power of tumor volume and regression ratio for patient subgroups stratified by lymph node status (Table 2). The p-values for outcome prediction were higher for the patient group with negative lymph nodes than those of the group with positive lymph nodes.

ROC analyses

The ROC method was used to determine the optimal cut-off points for each parameter for best outcome prediction. The ROC results are shown in Fig. 1 and the derived optimal thresholds are presented in Table 3. Parameter values for volumes and regression ratios larger than the cut-offs were associated with poor outcome. The values of the optimal cut-offs were fairly close for the two outcome endpoints LR and DOD (Table 3). Therefore, to streamline and simplify the predictors, only one set of cut-offs from LR predictions was used for further analyses for both the LR and the DOD prediction and to develop the predictive algorithms.

Prediction algorithms and their sensitivity and specificity

Based upon the cut-offs derived from ROC analyses, algorithms with combined parameters of volume and regression ratio at various time points were explored to identify patients at risk for LR and DOD. Judging by the sensitivity/specificity analyses, the following algorithms showed potential value for clinical application: (1) the regression ratio of MRI4 (V_4/V_1 > 10%); (2) the regression ratio of MRI3 ($V_3/V_1 > 20\%$); (3) the initial tumor volume and the ratio of MRI3 ($V_1 > 40\ cm^3$ and $V_3/V_1 > 20\%$); and (4) the initial tumor volume and the ratio of MRI2 ($V_1 > 40\ cm^3$ and $V_2/V_1 > 75\%$). The sensitivity and specificity, confidence intervals (CI), and accuracy of these four algorithms are summarized in Table 4. The efficacy of these algorithms was analyzed statistically, as well as the timing for outcome prediction.

Algorithm 3 (V_1 >40 cm^3 and V_3/V_1 >20%), based on the initial tumor volume V_1 and the volume regression ratio at MRI3 (4-5 weeks of RT), had a high sensitivity of 89%, a high specificity of 87%, and an accuracy of 88% for LR, and a sensitivity of 54%, a specificity of 83%, and an accuracy of 73% for DOD. Algorithm 4 (v_1 >40 cm^3 and V_2/V_1>75%), based on an earlier measurement of V_2 at MRI2 (2-3 weeks after RT start), showed a sensitivity of 61%, a specificity of 94%, and an accuracy of 86% for LR, and a sensitivity of 36%, a specificity of 90%, and an accuracy of 71% for DOD. Kaplan-Meier survival analysis for the two algorithms for LC and DSS are presented in Fig. 2. The p-values from the log-rank test show that the two algorithms ($p<0.001$) are highly significant during RT in identifying patients at risk for ultimate LR and DOD. For the best prediction with the algorithm 3 (V_1 >40 cm^3 and V_3/V_1>20%), the 5-year LC rates for the two separated groups differed by 63% (96% vs. 33%, $p<0.001$), and the 5-year DSS rates differed by 37% (75% vs. 38%, $p<0.001$). Similarly for the early prediction with algorithm 4 (V_1 >40 cm^3 and V_2/V_1>75%), the 5-year LC rates for the two identifiedgroups was 89% vs. 27% ($p<0.001$), and the 5-year DSS rate was 70% vs. 33% ($p=0.001$, Fig. 2).

Discussion

Advanced cervical cancer continues to be a disease with significant mortality [16, 17]. Once the tumor recurs after the completion of RT/CT, options for salvage therapy are poor, and outcome is almost uniformly fatal [18]. Therefore, the prediction of therapy outcome at the earliest possible time point before or during the initial treatment course is of eminent importance to optimize therapy regimens and increase the chance of cure for individual patients. If poor response to an ongoing standard therapy is predicted sufficiently early enough, a therapeutic window may be provided to modify the therapy strategy for better outcome.

Tumor size has long been established as an important prognostic factor in cervical cancer [5-8]. Numerous studies using tumor size estimated by clinical palpation have shown correlation with clinical outcome [5-8]. The use of 3D tumor volume measurements through quantitative imaging analysis with MRI has greatly improved the accuracy of tumor volume assessment [1-4] compared to clinical palpitation for tumor size estimation. This higher precision of tumor delineation enables not only more accurate pre-therapy measurement, but also serial measurements of tumor volume during and after the course of therapy [1, 2]. Tumor regression can be better quantified, and early results have shown that tumor regression correlates with outcome. Most such studies of tumor volume and outcome in cervical cancer have assessed tumors before therapy or after completion of therapy [9, 10, 13], and only a few have obtained intra-treatment measurements [11, 12]. With the large individual variations in initial tumor volumes and tumor regression rates of the reported data the best parameter threshold values and optimal timing for tumor volume measurement and it regression rate have not been well established for practical clinical translation.

With its largest patient number, longest follow-up of studies of this kind to date, and prospective serial imaging schedule, our study is well suited to identify promising MRI tumor volumetric parameters that are associated with radio-responsiveness, tumor control, and patient survival. Serial imaging at pre-therapy, week 2, week 5, and post-therapy has allowed us to evaluate and compare the sensitivity and specificity of the tumor regression metrics, as well as the absolute tumor volumes from the four serial measurements.

Our results suggest that a combination of tumor volume-related parameters, incorporating both the absolute tumor volume and tumor regression ratio, is necessary to increase the accuracy of outcome prediction. Although regression rate V_4/V_1 at post-RT time point (MRI4) had an accuracy of 93%, this accuracy was largely based on a high specificity and a

high tumor control rate in our patient data (Table 4). The combination of initial tumor volume information ($V_1 > 40\ cm^3$) and the earlier intra-treatment regression parameter ($V_3/V_1 > 20\%$, obtained at 40-50 Gy at 4-5 weeks of RT) improved the sensitivity of tumor recurrence prediction from 67% to 89% (Table 4). This finding suggests that regression rate alone may not fully assess the impact of absolute tumor cell number during the dynamic events of cytotoxicity-induced tumor reduction. For tumors with a small initial volume ($V_1 < 40\ cm^3$), the standard RT/CT is adequate to eradicate all tumor cells regardless the tumor regression rate, which may be influenced by either radiosensitivity or tumor perfusion. The algorithm with combined parameters ($V_1 > 40\ cm^3$ *and* $V_3/V_1 > 20\%$) identified patients with both large initial tumor volume ($V_1 > 40\ cm^3$) and radio-resistant tumor cells ($V_3/V_1 > 20\%$ indicating poor response at 40-50 Gy), who were likely to ultimately fail standard treatment, as shown by the poor LC rate of only 33% in the Kaplan-Meier analysis ($p<0.001$, Log-rank test, Fig. 2a). Similarly, for DSS, the addition of initial absolute volume $V_1 > 40\ cm^3$ improved the sensitivity of the post-therapy regression rate (V_4/V_1) from 36% to more than 54% with algorithm 3 ($V_1 > 40\ cm^3$ *and* $V_3/V_1 > 20\%$) and resulted in strong outcome correlation ($p<0.001$, Log-rank test, Fig. 2c). In these patients, the pre-RT parameter V_1 in combination with the mid-RT parameters ($V_3/V_1 > 20\%$) can be used to guide timely therapy intervention (e.g. radiation dose escalation or more intense, novel chemotherapy approaches) that may be necessary to overcome the compound challenge of large tumor burden and low radio-sensitivity.

Evaluation of the timing of volume measurement throughout the course of RT/CT showed that sensitivity and specificity generally increased at the later time points. For LR, while ROC analysis showed poor results for V_1 alone, ROC curves increasingly improved with volumes obtained later in the course of RT/CT (Fig. 1a). V_2 at 20-25 Gy (2 weeks of RT/CT) did not perform as well as V_3 at 40-50 Gy (4-5 weeks of RT/CT) and V_4 (1-2 months post-RT) (Fig. 1a). The mean of V_2 (50 cm^3) remained large and ranged widely (Table 1) early in the RT course at 20-25 Gy, while much greater volume decrease was evident later (V_3, V_4). The observation that later measurements in the RT course improved the predictive power of absolute volume may be explained by a lag time between the actual tumor cell kill and measurable tumor shrinkage by anatomical imaging. Although typically 99% of tumor cells are killed during the first 2 weeks of RT, morphologic tumor volume reduction is not measurable until cell clearance has occurred. The intra-treatment MRI scans reflect not only the radiation cell-killing, but also the effectiveness of dead cell clearance, which is, to a certain extent, related to the tumor micro-environment and fluid circulation [19, 20]. Later in the course of RT, after cell clearance from earlier cell-killing has occurred, the effect of cell-killing becomes more measurably evident. This may explain why the later V_3 and V_4 overall correlated better with outcome than the earlier V_2 (Table 2).

We expect that the post-RT volume V_4 is most likely dominated by the repopulation of residual tumor, as demonstrated in a separate modeling study [19, 20]. The information from both, tumor regression due to radiation cell-killing and tumor repopulation, may explain the high sensitivity of V_4 as a surrogate endpoint for LR. However the value of V_4 for clinical management is off-set by the late time point of post-therapy, when V_4 information is available.

While the parameters are also useful for the prediction of survival, their sensitivity and specificity for DOD were less optimal than those for LR (Tables 2 and 4, Figs. 1 and 2). This may be related to the fact that DOD is likely also determined by other biological or tumor micro-environmental factors, which may not be determined by local tumor bulk alone. Although sensitivities were lower, the algorithm combining pre-RT volume ($V_1 > 40\ cm^3$) and volume regression later in RT V_3 was effective in differentiating patients with DSS from those DOD (Table 4, Fig. 2).

When the patients were stratified by lymph node status (Table 2), the prediction power of tumor volume and regression ratio was higher for the patient group with negative lymph nodes than those of the other group with positive lymph nodes. It may be interpreted as the tumor volume and its regression provide a local measure of tumor response; therefore they provide a better prediction power of LC and DSS for patients with negative lymph node. The other reason might be the disparity of the patient numbers in the two groups (59 vs. 21 patients with negative and positive lymph node respectively).

Based upon the results of our current study, we would take the following approaches for future studies to validate these prognostic factors: (1) analyze larger database to validate the current findings; (2) refine and optimize the algorithms developed in the current study; (3) combine with functional MRI [21-26] to further improve the overall prediction power of clinical outcome. The overall imaging metric–outcome correlation results of our study confirm the value of serial MRI imaging in the assessment of tumor volume and monitoring of tumor regression/ response to the ongoing treatment. Our parameters provide a basis for development of algorithms to refine the efficacy of response assessment and to optimize outcome prediction. Such parameters show promise in classifying radio-responsiveness and predicting tumor control and patient survival in cervical cancer.

Conclusion

In conclusion, high-precision 3D MRI-based serial tumor measurements provide important information about subtle morphologic changes as the early therapy response to an ongoing treatment in individual patients. Our results with long-term follow-up data showed that the combined pre-therapy volumes and mid-RT volume regression ratios were highly accurate in predicting local failure and cancer death. Outcome prediction can be as early as 2 weeks, and the best prediction was at 4 weeks into the RT/CT treatment course. Therefore the algorithms developed in this study enable the early identification of patients who are at risk of treatment failure and may be benefited from more aggressive intervention.

Condensed abstract

In this study we investigated the efficacy of outcome prediction using serial MRI examinations to measure both tumor volumes and regression ratios before, during, and after radiotherapy and developed algorithms to identify early cervical cancer patients at risk of treatment failure.

Acknowledgments

Funding: The work was supported in part by the National Institutes of Health [R01 CA 71906].

References

1. Burghardt E, Hofmann HM, Ebner F, Haas J, Tamussino K, Justich E. Magnetic resonance imaging in cervical cancer: a basis for objective classification. Gynecol Oncol. 1989; 33(1):61–7. [PubMed: 2703168]
2. Greco A, Mason P, Leung AWL, Dische S, McIndoe GA, MC A. Staging of carcinoma of the uterine cervix: MR-surgical correlation. Clin Radiol. 1989; 40:401–05. [PubMed: 2758751]
3. Subak L, Hricak H, Powell CB, Azizi L, JL S. Cervical carcinoma: computed tomography and magnetic resonance imaging for preoperative staging. Obstet Gynecol. 1995; 86(1):43–50. [PubMed: 7784021]

4. Hricak H, Powell CB, Yu KK. Invasive cervical carcinoma: role of MR imaging in pretreatment work-up - cost-minimization and diagnosis efficacy. Radiology. 1996; 198:403–09. al e. [PubMed: 8596840]
5. Kovalic JJ, Perez CA, Grigsby PW. The effect of volume of disease in patients with carcinoma of the uterine cervix. Int J Radiat Oncol Biol Phys. 1991; 21:905–10. al e. [PubMed: 1917618]
6. Lowrey GC, Mendenhall MW, RR M. Stage IB or IIA-B carcinoma of the intact uterine cervix treated with irradiation: a multivariate analysis. Int J Radiat Oncol Biol Phys. 1992; 24:205–10. [PubMed: 1526856]
7. Perez CA, Grigsby P, Nene S. Effect of tumor size on the prognosis of carcinoma of the uterine cervix treated with irradiation alone. Cancer. 1992; 69:2796–806. al e. [PubMed: 1571911]
8. Eifel PJ. Problems with the Clinical Staging of Carcinoma of the Cervix. Semin Radiat Oncol. 1994; 4(1):1–8. [PubMed: 10717083]
9. Hricak H. Cancer of the uterus: the value of MRI pre-and post-irradiation. Int J Rad Oncol Biol Phys. 1991; 21:1089–94.
10. Flueckiger F, Ebner F, Poschauko H, Tamussino K, Einspieler R, G. R. Cervical cancer: serial MR imaging before and after primary radiation therapy - a 2-year follow-up study. Radiology. 1992; 184:89–93. [PubMed: 1609108]
11. Mayr NA, Magnotta VA, Ehrhardt JC, Wheeler JA, Sorosky JI, Wen BC, et al. Usefulness of tumor volumetry by magnetic resonance imaging in assessing response to radiation therapy in carcinoma of the uterine cervix. Int J Radiat Oncol Biol Phys. 1996; 35(5):915–24. [PubMed: 8751400]
12. Hatano K, Sekiya Y, Araki H, Sakai M, Togawa T, Narita Y, et al. Evaluation of the therapeutic effect of radiotherapy on cervical cancer using magnetic resonance imaging. Int J Radiat Oncol Biol Phys. 1999; 45(3):639–44. [PubMed: 10524417]
13. Sethi TK, Bhalla NK, Jena AN, Rawat S, R. O. Magnetic resonance imaging in carcinoma cervix--does it have a prognostic relevance. J Cancer Res Ther. 2005; 1(2):103–07. [PubMed: 17998636]
14. Hricak H, Lacey CG, Sandles LG, Chang YC, Winkler ML, Stern JL. Invasive cervical carcinoma: comparison of MR imaging and surgical findings. Radiology. 1988; 166(3):623–31. [PubMed: 3340756]
15. Glanz, SA. The Mann-Whitney rank-sum test. In: Jeffers, JD.; Englis, MR., editors. Primer of biostatistics. 3rd ed. McGraw-Hill, Inc.; New York: 1992. p. 262-334.
16. Rose PG, Blessing JA, Gershenson DM, McGehee R. Paclitaxel and Cisplatin as First-Line Therapy in Recurrent or Advanced Squamous Cell Carcinoma of the Cervix: A Gynecologic Oncology Group Study. JCO. 1999; 17:2676.
17. Eifel PJ, Winter K, Morris M, Levenback C, Grigsby PW, Cooper J, et al. Pelvic irradiation with concurrent chemotherapy versus pelvic and para-aortic irradiation for high-risk cervical cancer: an update of radiation therapy oncology group trial (RTOG) 90-01. J Clin Oncol. 2004; 22:872–80. [PubMed: 14990643]
18. Kastritis E, Bamias A, Efstathiou E, Gika D, Bozas G, Zorzou P, et al. The outcome of advanced or recurrent non-squamous carcinoma of the uterine cervix after platinum-based combination chemotherapy. Gynecol Oncol. 2005; 99:376–82. [PubMed: 16051322]
19. Wang JZ, Mayr NA, Yuh WTC, Montebello J, Zhang H, Gupta J, et al. Kinetic model of tumor regression during radiation therapy of cervical cancer. Int J Radiat Oncol Biol Phys. 2006; 66:S603.
20. Huang Z, Mayr NA, Yuh WTC, Lo SS, Montebello JF, Grecula JC, et al. Predicting outcomes in cervical cancer: a kinetic model of tumor regression during radiation therapy. Cancer Res. 2009 (accepted).
21. Semple SI, Harry VN, Parkin DE, Gilbert FJ. A combined pharmacokinetic and radiologic assessment of dynamic contrast-enhanced magnetic resonance imaging predicts response to chemoradiation in locally advanced cervical cancer. Int J Radiat Oncol Biol Phys. 2009; 75(2): 611–7. [PubMed: 19735887]
22. Liu Y, Bai R, Sun H, Liu H, Zhao X, Li Y. Diffusion-weighted imaging in predicting and monitoring the response of uterine cervical cancer to combined chemoradiation. Clin Radiol. 2009; 64(11):1067–74. [PubMed: 19822239]

23. Taieb S, Faivre-Pierret M, Nickers P, Lesoin A, Narducci F, Ceugnart L. Functional MR Imaging: new tool to predict outcome for cervical carcinoma of uterus treated by concomitant radiochemotherapy? Cancer Radiother. 2009; 13(6-7):511–4. [PubMed: 19717325]

24. Yuh WT, Mayr NA, Jarjoura D, Wu D, Grecula JC, Lo SS, et al. Predicting control of primary tumor and survival by DCE MRI during early therapy in cervical cancer. Invest Radiol. 2009; 44(6):343–50. [PubMed: 19661844]

25. Mayr NA, Wang JZ, Zhang D, Montebello JF, Grecula JC, Lo SS, et al. Synergistic effects of hemoglobin and tumor perfusion on tumor control and survival in cervical cancer. Int J Radiat Oncol Biol Phys. 2009; 74(5):1513–21. [PubMed: 19286329]

26. Mayr NA, Wang JZ, Zhang D, Grecula JC, Lo SS, Jaroura D, et al. Longitudinal Changes in Tumor Perfusion Pattern during the Radiation Therapy Course and its Clinical Impact in Cervical Cancer. Int J Radiat Oncol Biol Phys. 2009 (in press).

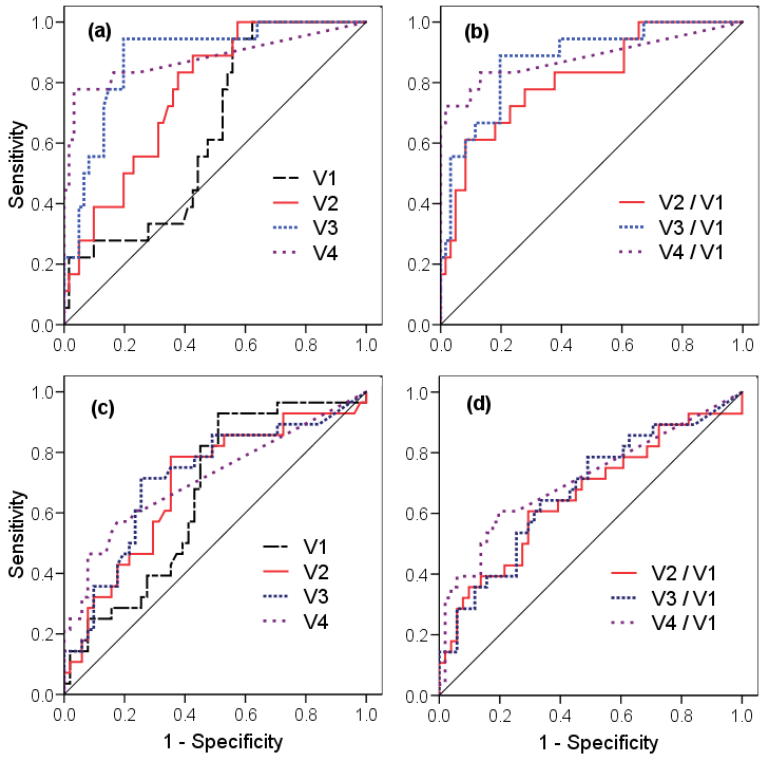

Fig. 1.

The ROC curves of (a) tumor volumes and (b) regression ratios for local recurrence of the tumor, and (c) tumor volumes and (d) regression ratios for dead of disease.

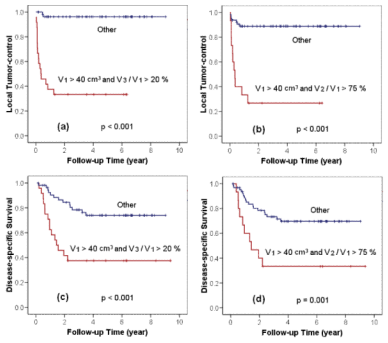

Fig. 2.

Kaplan-Meier actuarial analysis for local control of the tumor using (a) algorithm 3, the approach of best prediction, (b) algorithm 4, the approach of earliest prediction; and for disease-specific survival using (c) algorithm 3, (d) algorithm 4.

Cancer. Author manuscript; available in PMC 2011 November 1.

Table 1

Tumor volume categorized by clinical outcome of tumor local control and disease-specific survival

Therapy Outcome		Patient number	Tumor Volume (cm^3)	V_1	V_2	V_3	V_4
Local control	Yes	62	Range	3.4~342	0.4~248	0~48	0~13
			Mean ± Std	66±55	36±39	8.4±11.5	0.59±1.9
	No	18	Range	41~700	20~493	1.9~192	0~121
			Mean ± Std	130±162	96±119	47±52	26±36
Disease-specific survival	Yes	52	Range	7.3~342	1.3~248	0~48	0~18
			Mean ± Std	64±57	36±40	9±13	1±3
	No	28	Range	3.4~700	0.4~493	0.0~192	0~121
			Mean ± Std	111±133	76±100	31±46	16±32
Total patients		80	Range	3.4~700	0.4~493	0~192	0~121
			Mean ± Std	81±93	50±70	17±31	6.3±20

Note: V_1, V_2, V_3, and V_4 represent tumor volumes measured by MRI1, MRI2, MRI3, and MRI4 respectively.

Table 2

Prediction(p-value of Mann-Whitney rank-sum tests) of local control and disease-specific survival by absolute tumor volume (V_1, V_2, V_3, V_4) and regression ratio (V_2/V_1, V_3/V_1, V_4/V_1)for all patients and subgroups stratified by tumor stage and lymph node status.

Tumor Volume and Regression Ratio		**V_1**	**V_2**	**V_3**	**V_4**	**V_2/V_1**	**V_3/V_1**	**V_4/V_1**
All 80 patients	Local Control of Tumor	0.06	5×10^{-4}	1×10^{-6}	2×10^{-8}	7×10^{-5}	1×10^{-6}	1×10^{-8}
	Disease-Specific Survival	0.015	0.004	0.001	3×10^{-4}	0.03	0.009	3×10^{-4}
Patients Stratified by Tumor Stage								
Stage I, II (42 pat.)	Local Control of Tumor	0.16	0.07	0.02	0.002	0.29	0.08	0.003
	Disease-Specific Survival	0.17	0.14	0.03	0.003	0.77	0.24	0.004
Stage III, IVA (38 pat.)	Local Control of Tumor	0.78	0.06	8×10^{-5}	2×10^{-5}	9×10^{-4}	1×10^{-5}	8×10^{-6}
	Disease-Specific Survival	0.89	0.34	0.12	0.04	0.07	0.06	0.03
Patients Stratified by Lymph Node (LN) Status								
LN negative (59 pat.)	Local Control of Tumor	0.17	0.008	8×10^{-5}	2×10^{-5}	0.0018	1×10^{-4}	1×10^{-5}
	Disease-Specific Survival	0.07	0.048	0.017	0.010	0.11	0.03	0.008
LN positive (21 pat.)	Local Control of Tumor	0.16	0.02	0.004	0.0004	0.013	0.004	0.0004
	Disease-Specific Survival	0.15	0.047	0.04	0.02	0.14	0.13	0.02

Table 3

Optimal ROC cut-offs for outcome prediction (local tumor recurrence or dead of disease).

Endpoints	Tumor Volume (cm^3)				Regression Ratio (%)		
	V_1	V_2	V_3	V_4	V_2/V_1	V_3/V_1	V_4/V_1
Local Tumor Recurrence	40	20	11	3	75 %	20 %	10 %
Dead of Disease	43	34	9	2.5	65 %	15 %	7 %

Cancer. Author manuscript; available in PMC 2011 November 1.

Table 4

Sensitivity, specificity and accuracy of the developed algorithms to predict treatment failure (local tumor recurrence or dead of disease)

Prediction Algorithms		Sensitivity (%) (95% CI)	Specificity (%) (95% CI)	Accuracy rate (%)
Local Tumor Recurrence				
1	(V_4/V_1 >10%)	67 (41, 87)	100 (94, 100)	93
2	(V_3/V_1 >20%)	89 (65, 99)	79 (66, 88)	81
3	(V_1 >40 cm^3) & (V_3/V_1 >20%)	89 (65, 99)	87 (76, 94)	88
4	(V_1 >40 cm^3) & (V_2/V_1 >75%)	61 (36, 83)	94 (84, 98)	86
Dead of Disease				
1	(V_4/V_1 >10%)	36 (19, 56)	96 (87, 100)	75
2	(V_3/V_1 >20%)	54 (34, 72)	73 (59, 84)	66
3	(V_1 >40 cm^3) & (V_3/V_1 >20%)	54 (34, 72)	83 (70, 92)	73
4	(V_1 >40 cm^3) & (V_2/V_1 >75%)	36 (19, 56)	90 (79, 97)	71